Frontiers in Bioscience Landmark

Front. Biosci. (Landmark Ed) **2025**; 30(8): 39570
https://doi.org/10.31083/FBL39570

Original Research

Dendritic Cells Induce Clec5a-mediated Immune Modulation in MPTP-induced Parkinson's Disease Mouse Model

So-Yeon Choi[1,†], Ji-Hee Nam[1,†], Min-Seon Song[1], Jun-Ho Lee[1], Kyung-Eun Noh[1], Ji-Soo Oh[1], Nam-Chul Jung[1], Jie-Young Song[2], Dae-Seog Lim[1,*]

[1]Division of Life Sciences and Department of Life Science, Graduate School, CHA University, 13488 Seongnam-si, Gyeonggi-do, Republic of Korea
[2]Division of Radiation Biomedical Research, Korea Institute of Radiological and Medical Sciences, 01812 Seoul, Republic of Korea
*Correspondence: dslim@cha.ac.kr (Dae-Seog Lim)
[†]These authors contributed equally.

Academic Editors: Wei-Lin Jin and Hongquan Wang
Submitted: 7 April 2025 Revised: 10 July 2025 Accepted: 29 July 2025 Published: 30 August 2025

Abstract

Background: Parkinson's disease (PD) is characterized by a progressive decline in dopaminergic neurons within the substantia nigra (SN). Although its underlying cause has yet to be fully elucidated, accumulating evidence suggests that neuroinflammation contributes substantially to disease development. Treatment strategies targeting neuroinflammation could improve PD outcomes. Monocyte-derived tolerogenic dendritic cells (tolDCs) modulate immune responses and induce regulatory T cells (Tregs) during various inflammatory diseases. However, the mechanisms underlying tolDC-mediated immunoregulation in PD remain unclear. **Methods**: We investigated the immune modulatory role of tolDCs by analyzing gene expression patterns and identified that the C-type lectin domain family 5 member A (Clec5a) was highly induced in tolDCs. To assess its function, we generated Clec5a-knockdown tolDCs and measured cytokine production, including interleukin (IL)-10 and IL-6, forkhead box protein P3 (Foxp3)$^+$ Treg induction, and nuclear factor kappa B (NF-κB) signaling activity. Furthermore, we evaluated the therapeutic effects of Clec5a-expressing dendritic cells (DCs) in a 1-methyl-4-phenyl-1,2,3,6-tetrahydropyridine (MPTP)-induced PD mouse model. Dopaminergic neuron survival, α-synuclein (α-syn) accumulation, neuroinflammatory markers, and locomotor behavior were analyzed following DC administration. **Results**: Clec5a-knockdown tolDCs exhibited reduced immunomodulatory function and IL-10 levels but enhanced IL-6 levels. In addition, these cells induced fewer Foxp3$^+$ Tregs and showed significantly enhanced NF-κB signaling activity. In the MPTP-induced PD model, administration of Clec5a-expressing DCs ameliorated dopaminergic neuron loss and α-syn accumulation. Furthermore, Clec5a-expressing DCs reduced the number of CD45^{high}CD11b$^+$CD86$^+$ macrophages in the brain, reduced brain inflammatory cytokine expression, and improved locomotor activity. **Conclusions**: These findings suggest that Clec5a plays a critical role in the immunomodulatory function of tolDCs. The administration of Clec5a-expressing DCs effectively reduced neuroinflammation and protected dopaminergic neurons in an MPTP-induced PD model. Therefore, Clec5a-expressing tolDCs may demonstrate therapeutic potential by managing PD symptoms by suppressing inflammatory responses associated with neurodegeneration.

Keywords: dendritic cells; immune tolerance; Clec5a; regulatory T cells; Parkinson disease

1. Introduction

Parkinson's disease (PD) ranks as the second most common neurodegenerative disease globally and predominantly affects individuals of advanced age [1–3]. The clinical profile of PD encompasses both motor dysfunctions, such as resting tremors, bradykinesia, rigidity, and impaired postural reflexes, and various non-motor symptoms, all of which substantially contribute to morbidity [4]. These manifestations are largely driven by the progressive degeneration of nigrostriatal dopaminergic neurons and the intracellular aggregation of misfolded α-synuclein (α-syn) protein, leading to Lewy body pathology [5], and may also be exacerbated by genetic mutations such as leucine-rich repeat kinase 2 (LRRK2), which promotes endoplasmic reticulum (ER) stress through the thrombospondin 1 (THBS1)/transforming growth factor beta 1 (TGF-β1) axis [6]. In addition to neuronal mechanisms, recent insights have underscored a substantial role for immune-related processes in PD pathogenesis, involving crosstalk between innate and adaptive immunity [3,7]. Among these, microglial activation has been shown to facilitate neuroinflammatory cascades by releasing cytokines such as interleukin (IL)-6, tumor necrosis factor (TNF)-α, and interferon (IFN)-γ, thereby aggravating neuronal injury [8–11]. Moreover, aberrant infiltration of cluster of differentiation 4 (CD4)$^+$ T cells into the substantia nigra (SN) contributes to immune imbalance [12,13]. This occurs particularly by shifting the ratio of T helper type 1 (Th1)/T helper type 17 (Th17) cells relative to regulatory T cells (Tregs), which correlates with disease severity [14–18]. These findings collectively highlight the therapeutic potential of modulating CD4$^+$ T cell-mediated immune responses to improve neuroinflammation in PD [19,20].

Dendritic cells (DCs), as pivotal regulators of immune surveillance, specialize in presenting antigens (Ags) and initiating immune responses within both the peripheral and the central nervous system (CNS), where they continuously monitor and respond to immunological cues. Located near the cerebrospinal fluid, DCs can migrate to the draining cervical lymph nodes (LNs), where they may either exhibit tolerogenic capabilities or elicit immunogenic T-cell responses [21]. The objectives of DC-based therapy for PD are to promote Treg responses and induce tolerance against certain brain Ags [22]. By modulating immune responses against self-Ags, tolerogenic dendritic cells (tolDCs) serve as key modulators in immune-mediated diseases, including autoimmune and chronic inflammatory disorders such as rheumatoid arthritis [23,24], Type 1 diabetes [25,26], multiple sclerosis [27,28], and myocardial infarction [29,30]. Despite their therapeutic potential, tolDC-based therapies are challenging as the functionally distinct DC subsets need to be identified. Furthermore, due to the opposing functional characteristics of tolDCs and immunogenic mature DCs (mDCs), it is vital to identify the functional markers that can help distinguish between them. We previously performed gene profiling on mouse-derived tolDCs [31], which suggested that the C-type lectin domain family 5 member A (Clec5a) is uniquely overexpressed in tolDCs compared with other DC subsets.

Predominantly expressed on cells of the myeloid lineage, Clec5a, also known as myeloid DNAX-activating protein of 12 kDa (DAP12)-associating lectin 1 (MDL-1), interacts with the adaptor molecule DAP12 to initiate downstream signaling, which may result in either immunostimulatory or immunosuppressive responses depending on the cellular context [32–34]. Therefore, the dual functions of DAP12 may help explain the diverse roles of Clec5a in different cell types. Notably, some studies have suggested that Clec5a is involved in various immune responses, such as calcium mobilization, immunosuppressive leukocyte accumulation, and inflammatory cytokine production [35–38]. However, its specific role in DCs remains unclear. Moreover, the role of Clec5a expression in mediating the therapeutic effects of DCs in PD has not yet been investigated.

Therefore, this study evaluated the therapeutic effects of Clec5a-expressing tolDCs in 1-methyl-4-phenyl-1,2,3,6-tetrahydropyridine (MPTP)-induced PD mice, which is the most widely used animal model for PD [39–41]. We confirmed that tolDCs suppress neuroinflammation and attenuate PD-related dopaminergic neurodegeneration. We further observed that tolDCs enhanced forkhead box protein P3 (Foxp3)$^+$ Tregs and reduced the levels of inflammatory cytokines, including IL-1β and IL-6, in a Clec5a-dependent manner. These findings suggest that Clec5a-expressing tolDCs may serve as a potential Ag-specific immunotherapy for inflammatory diseases.

2. Materials and Methods

2.1 Animals

Male C57BL/6N mice (aged 6–8 weeks, weighing 14–16 g) were obtained from Orient Bio (Seongnam, Gyeonggi-do, Republic of Korea). They were kept in a controlled environment with a 12/12 h light/dark cycle and regulated temperature and humidity.

2.2 Lentiviral Constructs for Regulating Clec5a Gene Expression

To modulate Clec5a expression, a short hairpin RNA (shRNA) construct targeting the gene was synthesized by GenePharma (Shanghai, China). The sense sequence was inserted into the plasmid lentiviral knockout (pLKO)-shRNA-green fluorescent protein (GFP) vector. A control vector lacking the shRNA insert (pLKO-GFP) was used for comparison. The inserted shRNA sequence was as follows: 5′-CACCGGAACAGTCTGTCCCAGAAACTTCAAGAGAGTTTCTGGGACAGACTGTTCCTTTTTTG-3′.

2.3 Lentiviral Vector Production and Titration

The 293T cells (ATCC, CRL-3216, Manassas, VA, USA) were co-transfected with recombinant vectors and packaging plasmids (pRSV.Rev, pMDLg/pRRE, and pMD.G) using Lipofectamine™ 3000 Transfection Reagent (Invitrogen, Thermo Fisher Scientific, Waltham, MA, USA, Lot#2237579) for 4 h to generate lentivirus. Short tandem repeat (STR) profiling was used to validate 293T cells and confirm that they were free of mycoplasma. Post-transfection, the culture medium was replaced with fresh medium supplemented with GlutaMAX™ (Gibco, Thermo Fisher Scientific, Waltham, MA, USA, Lot#2360312) and sodium pyruvate (Gibco). After 24 h, the lentiviral supernatant was harvested, purified via ultracentrifugation, aliquoted, and stored at –80 °C. To determine viral titers, GFP-positive 293T cells were quantified by flow cytometry following exposure to serially diluted lentiviral vectors.

2.4 Generation of DCs and Transduction Using Lentiviral Vectors

Bone marrow-derived DCs were prepared from C57BL/6 mice euthanized with CO_2, following established protocols [42]. Bone marrow cells were isolated, dispersed into single-cell suspensions, and plated at 2×10^6 cells per 10 mL of culture medium. The medium contained RPMI 1640 (Cytiva, Hyclone Laboratories, Logan, UT, USA) with 10% fetal bovine serum (FBS; Corning, NY, USA), GlutaMAX™, antibiotic-antimycotic, 2-mercaptoethanol (Gibco), and 20 ng/mL recombinant mouse (rm) GM-CSF and IL-4 (JWCreaGene, Gwacheon, Gyeonggi-do, Republic of Korea). On day 3, an equal amount of fresh medium was added.

On day 5, the cells were transduced with lentiviral particles at a multiplicity of infection (MOI) of 6 in the

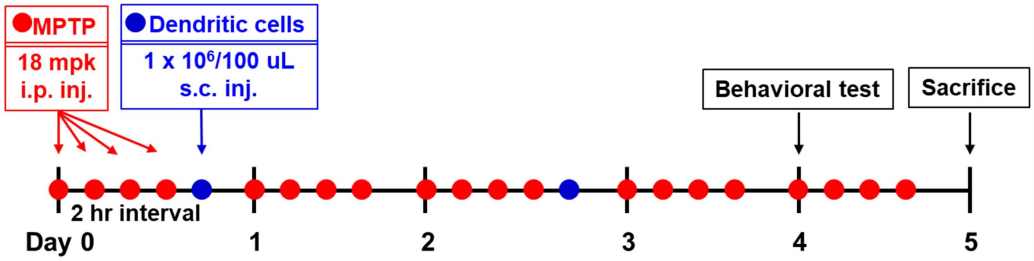

Fig. 1. Scheme of the experimental protocol. MPTP, 1-methyl-4-phenyl-1,2,3,6-tetrahydropyridine.

presence of 8 µg/mL polybrene (Santa Cruz Biotechnology, Dallas, TX, USA). After 24 h, the culture medium was replaced. For generation of tolDCs and Clec5a-knockdown tolDCs, the cells were stimulated on day 8 with 10 ng/mL TNF-α (BD Biosciences, San Jose, CA, USA) and 10 µg/mL keyhole limpet hemocyanin (KLH; Sigma-Aldrich, St. Louis, MO, USA) for 4 h. Conventional mDCs were produced by treating immature DCs (imDCs) with 1 µg/mL lipopolysaccharide (LPS) and 10 µg/mL KLH (Sigma-Aldrich) for 24 h. For *in vivo* use, KLH was replaced with 10 µg/mL rm α-syn (rPeptide, Watkinsville, GA, USA). All DC subsets were collected simultaneously, and their supernatants were harvested for cytokine analysis.

2.5 Generation of an MPTP-induced PD Mouse Model and tolDC Administration

The experimental design is summarized in Fig. 1. MPTP-HCl (18 mg/kg of free base; Sigma-Aldrich, #M0896) was intraperitoneally injected into the mice four times at 2 h intervals for 5 days [43]. The control animals received only phosphate-buffered saline (PBS). On days 0 and 2, 2 h after the last MPTP injection, the mice were subcutaneously injected at the back of the neck with 1×10^6 DCs. These cells were validated by STR profiling and verified to be mycoplasma-free before use in animal experiments. On day 5 following MPTP injection, Avertin (500 µL/mouse; 20 mg/mL) was intraperitoneally injected and the mice were subsequently CO_2 euthanized. Euthanasia was performed using the gradual-fill method. CO_2 was administered at a flow rate equivalent to approximately 10% of the 57 L chamber volume per minute (5.7 L/min), allowing for a gradual increase in CO_2 concentration. Upon confirmation of loss of consciousness, the flow rate was increased to 8 L/min (~14%/min) to complete the euthanasia process. This procedure was conducted in accordance with the American Veterinary Medical Association (AVMA) Guidelines for the Euthanasia of Animals. To remove blood and leukocytes from the brain's vasculature, the spleen and LNs were removed, and the mice were transcardially perfused with ice-cold 0.9% saline.

2.6 Clinical Parkinson's Disorder Score

The clinical symptoms of PD, which include chronic neurodegeneration with features indicating core motor function disruption, as well as behavioral symptoms, are challenging to reproduce in a mouse model [39]. Thus, we established a score based on the motor dysfunctions described in an MPTP-induced monkey model [44]. PD progression was assessed through daily observations in the home cage. The PD score was calculated by summing the scores of each of the four components (**Supplementary Table 1**).

2.7 Behavioral Analysis

2.7.1 Stepping Test

On day 4, three types of behavioral experiments were performed. The forepaw stepping adjustment test is a widely accepted method for evaluating forelimb akinesia in mice. During the procedure, the mouse's hindlimbs were gently elevated by lifting its tail, ensuring that only the forepaws remained in contact with the surface. The animal was then guided backward by the tail for a distance of 1 m at a consistent speed over approximately 3–4 s. The entire process was recorded on video, and the number of adjusting steps made by each forepaw was subsequently analyzed.

2.7.2 Pole Test

The pole test was conducted by positioning the mice head-upward at the top of a vertical wooden pole (50 cm in length and 1 cm in diameter) situated within their home cages. Before testing, mice underwent a 2-day training period, during which they completed three trials per day. On the test day, each mouse performed three additional trials, and the mean time required to execute a complete 180° turn (T-turn) and descend to the cage floor was measured. To prevent physical fatigue, cutoff times were established at 90 s for the T-turn and 180 s for the total descent. In cases where the mice fell while turning, the maximum time was recorded.

2.7.3 Tremor Test

The tremor assessment was performed by a blinded researcher. To measure the tremor amplitude, brief video recordings (8–10 s) of mice positioned on a small platform were obtained, consisting of approximately 60 consecutive frames. These frames were merged into a smart object, and the "mean" stack mode in Adobe Photoshop software

v.25.12.3 (Adobe Inc., San Jose, CA, USA) was used to integrate the motion into a single composite image. This approach allowed for the visualization of the displacement of the spine across frames, with the images inverted to enhance clarity. The image contrast was then analyzed using pixel intensity measurements in ImageJ v.1.53t (National Institutes of Health, Bethesda, MD, USA, https://imagej.net) to determine the degree of sharpness.

2.8 Immunofluorescence Staining of Tyrosine Hydroxylase (TH)-positive Neurons

On day 5, following MPTP injection, mouse brains were collected post-perfusion, as previously described. The brain tissue was immersed overnight in 4% paraformaldehyde (PFA) in PBS for fixation. Samples were subsequently equilibrated in 15% and 30% sucrose solutions for at least 16 h. Using a cryostat Leica CM3050 S (Leica Biosystems, Nussloch, Germany), the brains were coronally sliced into 30 µm-thick sections and preserved at –20 °C in a cryoprotectant medium until further analysis. For immunofluorescence staining, every sixth section encompassing the SN was selected. To prevent nonspecific interactions, frozen sections were pretreated in PBS containing 3% goat serum and 1% Triton™ X-100 (MilliporeSigma, Burlington, MA, USA) for 30 min. The tissue sections were then incubated overnight at 4 °C with a primary mouse anti-TH antibody (Invitrogen). The next day, the sections were incubated for 2 h at ambient temperature with a fluorescein isothiocyanate (FITC)-conjugated goat anti-mouse IgG secondary antibody (Jackson ImmunoResearch, West Grove, PA, USA). Afterward, the sections were washed three times with PBS (5 min per wash). Fluorescent signals were acquired using a Leica fluorescence microscope (Leica Microsystems, Wetzlar, Germany), and TH-positive cells were quantified using LAS AF imaging software v.4.0 (Leica Microsystems). Antibody information is provided in **Supplementary Table 2**.

2.9 Immunofluorescence Staining for Clec5a

DCs were seeded onto coverslips pre-coated with poly-L-lysine (MilliporeSigma) and subsequently fixed in 1% PFA in PBS for 10 min. Following fixation, the cells were permeabilized with 0.1% Triton™ X-100 in PBS, followed by washing with 0.05% Tween 20 in PBS (PBST; Daejung Chemicals & Metals, Siheung, Gyeonggi-do, Republic of Korea). To minimize nonspecific interactions, the cells were incubated with 5% normal goat serum for 30 min at room temperature. Subsequently, an anti-Clec5a antibody (R&D Systems, Minneapolis, MN, USA) was applied for an overnight incubation at 4 °C. The next day, the cells were treated with an Alexa Fluor 594-conjugated anti-mouse IgG antibody (Jackson ImmunoResearch) in antibody diluent (Agilent Technologies, Santa Clara, CA, USA) for 2 h at room temperature. After multiple washes with PBST, the coverslips were mounted using Fluoroshield™ containing DAPI (Sigma-Aldrich). Imaging was conducted using a TCS NT/SP confocal microscope (Leica) equipped with argon, krypton, and helium/neon lasers. **Supplementary Table 2** summarizes the antibodies used in this study.

2.10 Flow Cytometric Immunophenotyping of DCs

Phenotypic analysis involved direct immunofluorescence staining of the DC surface markers. The cells were stained using the following antibodies at 4 °C for 20 min: allophycocyanin (APC)-conjugated anti-CD11c (BioLegend, San Diego, CA, USA) and phycoerythrin (PE)-conjugated anti-CD11c (Invitrogen), PE-conjugated anti-CD40 (BD Biosciences), anti-CD80 (Invitrogen), anti-major histocompatibility complex (MHC) class II (BD Biosciences), anti-IL-10 (BD Biosciences), FITC-conjugated anti-CD14 (BioLegend), anti-CD54 (BD Biosciences), anti-CD86 (BioLegend), anti-MHC class I (BioLegend), propidium iodide (PI; BD Biosciences), and corresponding isotype controls. The cells were analyzed using a NovoCyte 3005 (ACEA Biosciences, Agilent Technologies, San Diego, CA, USA), and the data were analyzed using the FlowJo v.10 software (FlowJo, Ashland, OR, USA). All antibody information is presented in **Supplementary Table 3**.

2.11 Cytokine Measurement

On day 5, following MPTP injection, the perfused mouse brains were harvested as described above. For *in vivo* experiments, the brain tissue was lysed using the PROPREP™ protein extraction kit (iNtRON Biotechnology, Seongnam, Gyeonggi-do, Republic of Korea, #17081). The total protein concentration of the lysate was measured using a Pierce™ Bradford Plus Protein Assay Kits (Thermo Fisher Scientific, #23236). Cytokine levels were quantitated using commercial enzyme-linked immunosorbent assay (ELISA) kits following the manufacturer's protocols. For *in vitro* experiments, cytokine levels—including IL-1β, IL-4, IL-6, and TNF-α (BioLegend); IL-10, IL-12p40, and IFN-γ (BD Biosciences); and TGF-β (R&D Systems)—secreted by DCs or T cells were measured using commercially available ELISA kits.

2.12 Carboxyfluorescein Succinimidyl Ester (CFSE) T Cell Proliferation Assay

Spleens from mice were harvested and dissociated in RPMI 1640 medium. To enrich $CD3^+$ T cells, splenocytes were applied to nylon wool fibers (Polysciences, Inc., Warrington, PA, USA) according to the manufacturer's protocol. The purified T cells were labeled with a CFSE labeling kit (65-0850-84, Invitrogen, Waltham, MA, USA) and subsequently co-cultured with DCs at a 1:10 ratio (DC:T cells). $CD3^+$ T cells (1×10^6 cells/mL) and DCs (1×10^5 cells/mL) were incubated in 2 mL of RPMI 1640 medium supplemented with 10% FBS at 37 °C for 72 h. In this assay, T cells acted as responder cells, with DCs serving as stimulators.

2.13 Intracellular Cytokine Staining of the $CD4^+$ T-cell Subsets

To assess T cell subsets, surface markers were stained with APC-conjugated anti-CD4 (BioLegend) and FITC-conjugated anti-CD25 (BD Biosciences), followed by incubation at 4 °C for 20 min. The cells were subsequently fixed and permeabilized using either the BD Intracellular Staining Kit (554722/554723, BD Biosciences, San Jose, CA, USA) or the Foxp3/Transcription Factor Staining Buffer Set (00-5523-00, Invitrogen, Waltham, MA, USA). Intracellular staining was performed with PE-conjugated anti-IFN-γ (BD Biosciences), PE-conjugated anti-IL-17A (BioLegend), PE-conjugated anti-Foxp3, and Alexa Fluor 488-conjugated anti-IL-4 (Invitrogen). Flow cytometric analysis was conducted on a NovoCyte 3005, and data were processed using FlowJo software v.10. The antibodies used in the flow cytometry are listed in **Supplementary Table 3**.

2.14 Quantitative Real-time PCR (qRT-PCR)

Total RNA was extracted using Labozol (CMRZ001, Cosmogenetech, Seoul, Republic of Korea), and cDNA was synthesized with the LaboPass cDNA synthesis kit (CMRTK002, Cosmogenetech) according to the manufacturer's instructions. Quantitative real-time PCR was performed using Clec5a-specific primers and SensiFast™ SYBR® Hi-Rox Mix (Bioline, Memphis, TN, USA). The primer sequences were: Clec5a forward, 5′-TCTGCTGTATTTCCCACAGG-3′; Clec5a reverse, 5′-TTCGTCATTTCTCCCAAAGA-3′; glyceraldehyde-3-phosphate dehydrogenase (GAPDH) forward, 5′-AACAGCAACTCCCACTCTTC-3′; and GAPDH reverse, 5′-CCTGTTGCTGTAGCCGTATT-3′. Gene expression was normalized to GAPDH and analyzed in triplicate (Relative expression levels were calculated using the $2^{-\Delta\Delta CT}$ method with GAPDH as the reference gene).

2.15 Western Blotting

Protein quantification of whole-cell lysates from DCs was performed using the Pierce™ Bradford Plus Protein Assay Kits following lysis with the PRO-PREP™ protein extraction solution (iNtRON Biotechnology). Equal amounts of protein were loaded and separated by sodium dodecyl sulfate polyacrylamide gel electrophoresis (SDS-PAGE) and then transferred to polyvinylidene fluoride (PVDF) membranes (Thermo Fisher Scientific). The membranes were blocked in 10% skim milk (w/v) prepared in PBST and subsequently incubated overnight at 4 °C with the following primary antibodies: Clec5a, phosphorylated (p)-extracellular signal-regulated kinase (Erk)1/2, Erk1/2, p-nuclear factor kappa B (NF-κB) p65, NF-κB p65, p-c-Jun N-terminal kinase (JNK), JNK, p-p38, p38, p-signal transducer and activator of transcription (STAT)3, STAT3, p-spleen tyrosine kinase (Syk), and Syk (all purchased from Cell Signaling Technology, Danvers, MA, USA); DAP12 (Santa Cruz Biotechnology); and GAPDH (Bioss, Woburn, MA, USA). After washing, the membranes were incubated at room temperature for 2 h with appropriate horseradish peroxidase (HRP)-conjugated secondary antibodies, such as goat anti-mouse, mouse anti-goat, or mouse anti-rabbit IgG (Santa Cruz Biotechnology). Protein signals were detected using the SuperSignal™ Chemiluminescence Substrate (Thermo Fisher Scientific) and captured with a luminescence imaging system (ImageQuant LAS 4000; GE Healthcare, Chicago, IL, USA). Detailed antibody information is provided in **Supplementary Table 2**.

2.16 CNS Leukocyte Isolation

On day 5, after MPTP injection, the perfused mouse brains were harvested as described above. Percoll® (Sigma-Aldrich) was used for leukocyte isolation, according to the manufacturer's instructions. Briefly, the brains were gently homogenized and pelleted. The homogenates were resuspended in 37% isotonic Percoll®. A discontinuous isotonic Percoll® density gradient consisting of 70%, 37%, 30%, and 0% layers was prepared. The gradient was centrifuged at 300 $\times$g for 40 min at room temperature. Microglia and leukocytes were collected from the 37%/70% interface. The isolated cells were subjected to flow cytometric analysis to verify cellular identity based on their surface marker expression. All cell preparations tested negative for mycoplasma contamination. Detailed products information is provided in **Supplementary Table 4**.

2.17 Statistical Analysis

All experimental procedures were performed in at least three independent replicates. Data are expressed as the mean $\pm$ standard deviation (SD). To determine whether the data followed a normal distribution, the Shapiro–Wilk test was conducted. For comparisons between the two groups, the Student's *t*-test was applied when the data met the parametric assumptions, while the Mann–Whitney U test was used for nonparametric datasets. When comparing three or more independent groups, one-way ANOVA with a subsequent Tukey–Kramer post hoc test was used for normally distributed data. In contrast, for nonparametric comparisons involving multiple groups, the Kruskal–Wallis test was utilized, followed by pairwise testing adjusted with the Bonferroni correction. Survival analyses were performed using the Kaplan–Meier method (InStat; GraphPad Software, La Jolla, CA, USA). A *p*-value of less than 0.05 was considered to indicate statistical significance.

3. Results

3.1 Neuroprotective Effect of tolDCs in MPTP-intoxicated Mice

To evaluate the therapeutic effects of tolDCs, we administered either tolDCs or mDCs to MPTP-intoxicated mice. On day 5, the tolDC-treated mice (MPTP + tolDC) exhibited a higher survival rate compared with the mDC-treated (MPTP + mDC) or MPTP-intoxicated (MPTP)

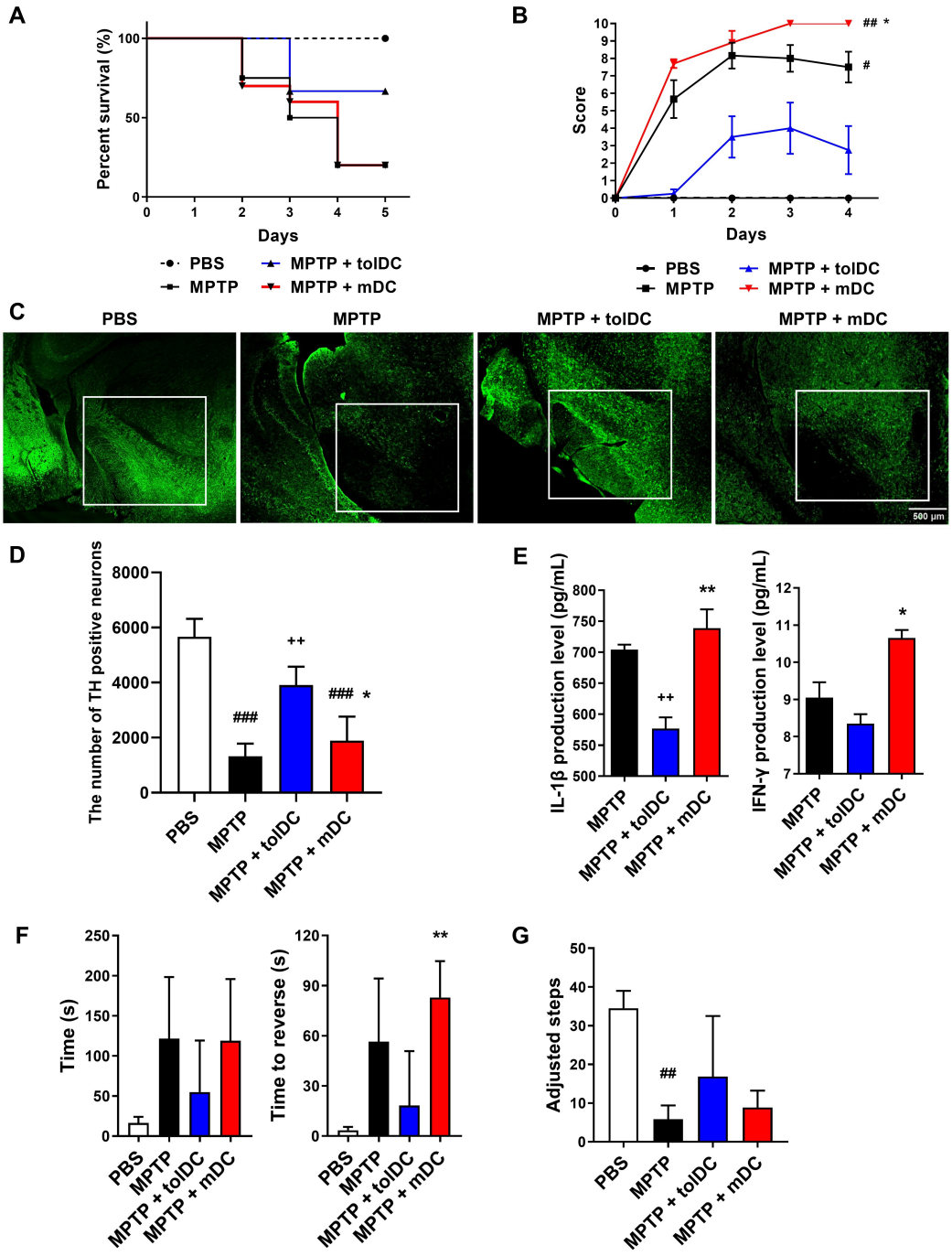

Fig. 2. Neuroprotective effect of tolerogenic dendritic cells (tolDCs). (A) Survival rates. Kaplan–Meier survival analysis in the phosphate-buffered saline (PBS) (n = 10), MPTP (n = 20), MPTP + tolDC (n = 10), and MPTP + mDC (n = 10) groups. tolDCs and mature DCs (mDCs) were generated by treatment with α-synuclein (α-syn). (B) Plots depicting disease severity. A scale from 0 to 10 was used to grade the severity of the disease (**Supplementary Table 1**) ($^{\#}p < 0.05$ and $^{\#\#}p < 0.01$ vs. PBS; $^{*}p < 0.05$ vs. MPTP + tolDC). (C) Tyrosine Hydroxylase (TH)-expressing dopaminergic neurons in substantia nigra pars compacta (SNpc) were visualized via Immunofluorescence imaging (TH; a marker of dopamine neurons); Representative images are displayed. Scale bar: 500 µm. (D) Quantification of TH-positive neurons in the substantia nigra (SN) region (Tukey–Kramer ANOVA; n = 3; $^{\#\#\#}p < 0.001$ vs. PBS; $^{++}p < 0.01$ vs. MPTP; $^{*}p < 0.05$ vs. MPTP + tolDC). (E) Cytokine profile of the brain. Bar plots illustrating the levels of interleukin (IL)-1β and interferon (IFN)-γ in the brain measured by enzyme-linked immunosorbent assay (ELISA) (Kruskal–Wallis ANOVA; n = 3; $^{++}p < 0.01$ vs. MPTP; $^{*}p < 0.05$ and $^{**}p < 0.01$ vs. MPTP + tolDC). (F) Pole test measuring descent time and reversal initiation (Kruskal–Wallis ANOVA; n $\geq$ 5; $^{**}p < 0.01$ vs. MPTP + tolDC). (G) Stepping test counting adjusted forelimb steps (Kruskal–Wallis ANOVA; n = 6; $^{\#\#}p < 0.01$ vs. PBS). All data are expressed as the mean $\pm$ SD.

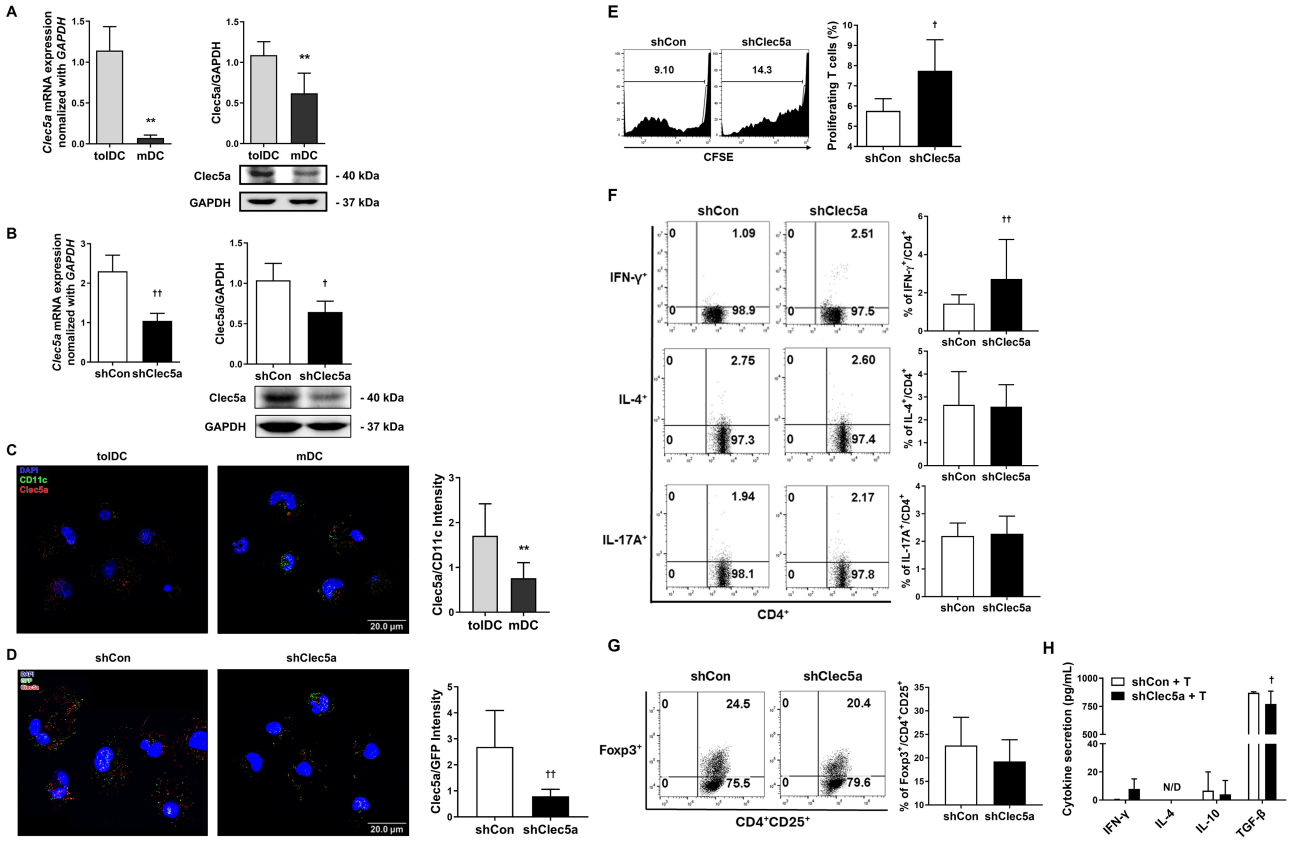

Fig. 3. C-type lectin domain family 5 member A (Clec5a) expression is affected by the immune response in tolDCs. (A) Clec5a mRNA levels were quantified using quantitative real-time PCR (qRT-PCR) (left; Mann–Whitney U test; n = 6 independent DC samples; $^{**}p < 0.01$ vs. tolDC), and protein expression was assessed by western blotting (right; Student's *t*-test; n = 6 independent DC samples; $^{**}p < 0.01$ vs. tolDC). Expression levels were normalized against glyceraldehyde-3-phosphate dehydrogenase (GAPDH). (B) Clec5a expression in shRNA-transduced dendritic cells (DCs) was analyzed by qRT-PCR (left; Student's *t*-test; n = 4 independent DC samples; $^{\dagger\dagger}p < 0.01$ vs. shCon) and western blotting (right). The bar graph presents the fold changes relative to immature DCs (imDCs) from at least four independent samples (Student's *t*-test; n = 4 independent DC samples; $^{\dagger}p < 0.05$ vs. shCon). (C) Immunofluorescence imaging visualized CD11c (green) and Clec5a (red) expression in DCs, with nuclei counterstained using DAPI (blue) (Mann–Whitney U test; n = 5 independent DC samples; $^{**}p < 0.01$ vs. tolDC). Scale bar: 20 μm. (D) Immunofluorescence analysis confirmed Clec5a (red) and green fluorescent protein (GFP) (green) expression, indicating the transduction efficiency. Nuclei were counterstained using DAPI (blue), and all images were acquired under consistent microscope settings (Mann–Whitney U test; n = 6; $^{\dagger\dagger}p < 0.01$ vs. shCon). Scale bar: 20 μm. (C) and (D) represent montages of representative single-cell confocal images, not continuous confocal fields. (E) shClec5a-mediated T cell proliferation was assessed by flow cytometry. Representative histograms and bar graphs show the percentage of proliferating $CD3^+$ T cells (Mann–Whitney U test; n = 6 independent samples; $^{\dagger}p < 0.05$ vs. shCon). (F,G) shClec5a-mediated T cell polarization was determined by flow cytometry. The proportions of Th (F) and Treg (G) are presented. Representative histograms and bar graphs indicate the proportion of each T cell subset (Mann–Whitney U test; n = 13; $^{\dagger\dagger}p < 0.01$ vs. shCon). (H) Cytokine secretion profiles of T cells stimulated with shClec5a were analyzed (Student's *t*-test; n ≥ 3 independent samples; $^{\dagger}p < 0.05$ vs. shCon). All data are presented as the mean ± SD.

groups (Fig. 2A). Disease progression was monitored over time across all groups. Compared with the MPTP group, the MPTP + tolDC group displayed a lower Parkinson's score, whereas the MPTP + mDC group showed the highest score (Fig. 2B). To investigate whether tolDCs exerted neuroprotective effects in the experimental PD model, dopaminergic neuronal degeneration in the substantia nigra pars compacta (SNpc) was analyzed using immunofluorescence staining. MPTP administration reduced TH-positive dopaminergic neuron numbers in the SN compared with the PBS-treated mice. While MPTP + tolDC significantly preserved dopaminergic neurons, the neuronal loss was

comparable between the MPTP + mDC and MPTP groups (Fig. 2C,D). To determine whether the injected DCs modulated inflammation in the MPTP-intoxicated mouse brains, we measured the levels of IL-1β and IFN-γ in whole brain lysates. These cytokines are functionally crucial for the activation of microglia and the exacerbation of symptoms in experimental PD models [45,46]. The expression of IL-1β and IFN-γ was lower in the MPTP + tolDC group, while the highest levels were detected in the MPTP + mDC group (Fig. 2E). Regarding behavioral tests, tolDC-treated mice performed better in the pole test, exhibiting shorter T-turn and total descent times (Fig. 2F). Improved performance in the stepping test (Fig. 2G) further supported the attenuation of motor deficits. Collectively, these findings indicate that tolDCs may confer neuroprotective benefits in MPTP-intoxicated mice.

3.2 Clec5a is Upregulated in tolDCs and Affects the T Cell-mediated Immune Response

The therapeutic potential of tolDCs in MPTP-treated mice was assessed in comparison with that of mDCs. *In vitro* analyses of tolDC-mediated immune responses revealed reduced levels of co-stimulatory molecules and proinflammatory cytokines relative to mDCs (**Supplementary Fig. 1A,B**). Conversely, the expression of IL-10, a representative anti-inflammatory cytokine, was elevated in tolDCs compared with that in mDCs (**Supplementary Fig. 1C**). Moreover, tolDCs had a lower proliferative capacity than mDCs but promoted the Th2 and Treg populations in the co-culture experiments (**Supplementary Fig. 1D–G**). These results suggest that tolDCs efficiently induced immune tolerance by suppressing inflammatory cytokine production and enhancing the proportion of Tregs.

Next, we examined the functional markers in DC subsets to determine the basis for the functional differences between tolDCs and mDCs. As Clec5a is upregulated in tolDCs [31], we generated tolDCs and mDCs to determine whether tolDCs expressed Clec5a by employing quantitative real-time PCR (qRT-PCR). The results indicated that Clec5a was significantly overexpressed in tolDCs compared with mDCs. In addition, western blot analysis of whole cell lysates showed enhanced Clec5a levels in tolDCs (Fig. 3A).

To investigate the functional significance of Clec5a in tolDCs, lentiviral transduction with Clec5a-targeting shRNA was employed. The Clec5a knockdown efficiency was verified through qRT-PCR and western blotting (Fig. 3B). Immunofluorescence analysis further revealed that Clec5a was strongly expressed on the surface of tolDCs (Fig. 3C) and was significantly downregulated in the Clec5a-knockdown tolDCs (shClec5a). Additionally, the transduction of lentiviral vectors was confirmed by GFP expression in DCs (Fig. 3D). We next evaluated whether Clec5a knockdown affected tolDC function. The results demonstrated that although Clec5a did not influence the expression of surface molecules, it markedly induced the production of IL-6 while decreasing the expression of IL-10 in tolDCs (**Supplementary Fig. 2A–C**). To evaluate the impact of shClec5a on T cell activation, DCs were co-cultured with $CD3^+$ T cells. Compared with shCon, T cell proliferation (Fig. 3E) and the $CD4^+IFN\text{-}\gamma^+$ Th1 population were significantly increased, whereas the Th2/Th17 populations remained similar to those in the shCon group (Fig. 3F). Moreover, shClec5a reduced the Treg population and TGF-β secretion (Fig. 3G,H). These results suggest that adaptive cellular immune responses, particularly Th1 and Treg-mediated immune responses, were affected by Clec5a levels.

3.3 Changes in NF-κB and STAT3 Activation via the Regulation of Clec5a Expression

The key downstream molecules were assessed to explore the signaling mechanisms underlying Clec5a-mediated immune regulation. In Clec5a-knockdown tolDCs, the expression of DAP12 and phosphorylated Syk was slightly reduced (Fig. 4A). While the phosphorylation of Erk, p38, and JNK remained unchanged between the shCon and shClec5a groups, STAT3 phosphorylation significantly declined, and NF-κB phosphorylation was markedly elevated in the shClec5a group (Fig. 4B). These results indicate that Clec5a contributes to the tolDC-based immune response via the NF-κB and STAT3 signaling pathways.

3.4 Neuroprotective Effect of Clec5a-expressing tolDCs in MPTP-intoxicated Mice

To determine whether the modulation of Clec5a expression in tolDCs influenced their therapeutic efficacy against PD, we administered Clec5a-expressing tolDCs to MPTP-intoxicated mice. The experimental protocol was the same as described previously. Kaplan–Meier analysis indicated enhanced survival in the tolDC-treated mice (MPTP + tolDC) compared with that in the mDC-treated (MPTP + mDC), shClec5a-treated (MPTP + shClec5a), or MPTP-intoxicated (MPTP) mice on day 5 (Fig. 5A). Disease severity increased with time in all experimental groups, whereas the MPTP + shClec5a group exhibited the highest Parkinson's score compared with the MPTP group (Fig. 5B). Compared with the MPTP group, although MPTP + tolDC ameliorated the loss of dopaminergic neurons, the loss was greater or similar in the MPTP + mDC and MPTP + shClec5a groups (Fig. 5C,D). In the SN region, α-syn levels were highest in the MPTP + mDC group, followed by the MPTP and MPTP + shClec5a groups (Fig. 5E). We next measured the levels of proinflammatory cytokines in whole brain lysates. The lowest IL-1β and IFN-γ levels were identified in the MPTP + tolDC group (Fig. 5F). Although the results were consistent among individuals, the T-turn and pole test times and the forepaw step counts were

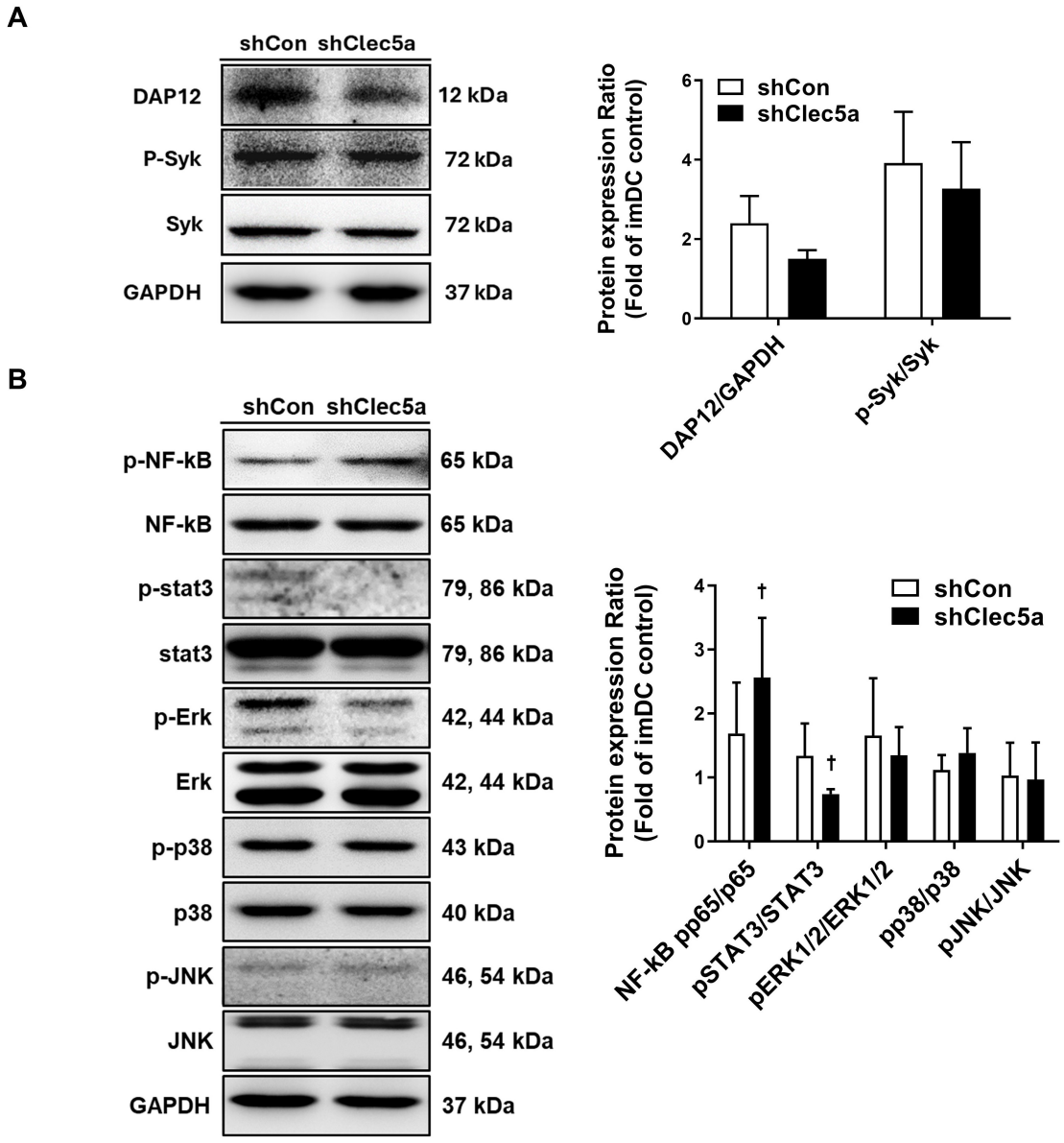

Fig. 4. Cell signaling analysis of shClec5a. (A) Western blotting was conducted to assess the expression of DNAX-activating protein of 12 kDa (DAP12), p-spleen tyrosine kinase (Syk), and Syk. The p-Syk expression was normalized to that of Syk. The corresponding bar graphs indicate the fold changes relative to imDCs (Mann–Whitney U test, n = 3). (B) Western blot analysis was also performed for key signaling proteins, including nuclear factor kappa B (NF-κB), signal transducer and activator of transcription (STAT)3, extracellular signal-regulated kinase (Erk)1/2, p38, and c-Jun N-terminal kinase (JNK). Phosphoprotein expression was normalized to the total expression of each protein. The bar graph represents the fold changes relative to imDCs (Mann–Whitney U test, n = 3; $^{\dagger}p < 0.05$ vs. shCon). All data are presented as the mean $\pm$ SD.

similar in the MPTP + shClec5a and MPTP + mDC groups; the MPTP + tolDC group exhibited minimal bradykinesia or motor dysfunction (Fig. 5G,H). The MPTP + tolDC group exhibited the lowest degree of tremors, whereas the MPTP + shClec5a and MPTP groups showed similar results (Fig. 5I and **Supplementary Fig. 3**). Taken together, these results imply that the modulatory effects of tolDCs on inflammation and motor dysfunction in MPTP-intoxicated mice depend on Clec5a expression levels.

3.5 Clec5a-expressing tolDCs Modulate Brain Immune Cells in MPTP-intoxicated Mice

To determine the *in vivo* effects of tolDC treatment on the brain and systemic immune systems, the mice were euthanized, and their spleens, LNs, and perfused brains were isolated. Flow cytometry analysis measured the proportions of Tregs (Fig. 6A) and M1/M2 macrophages (Fig. 6B) in the brain tissue after tolDC administration. The percentages of $CD4^{+}CD25^{+}Foxp3^{+}$

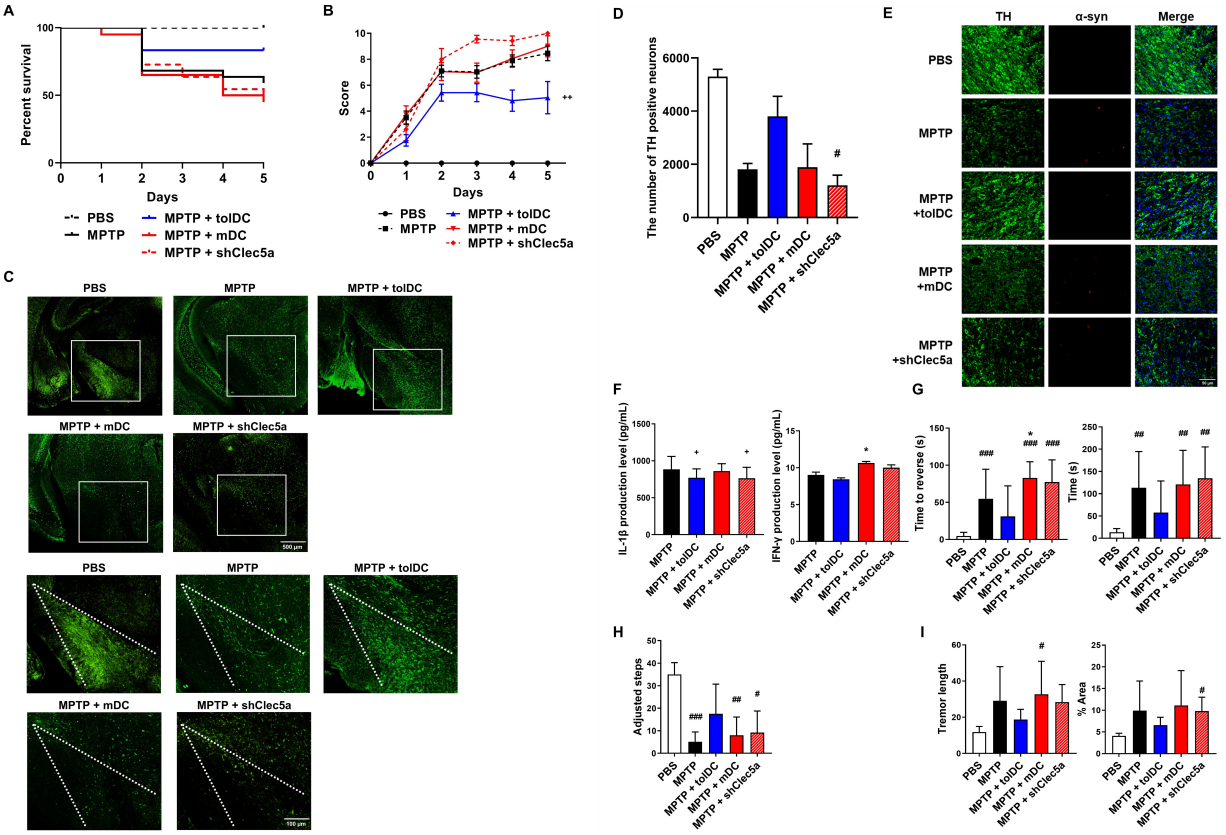

Fig. 5. Neuroprotective effects of Clec5a-expressing DCs. (A) Survival rates. Kaplan–Meier survival analysis in PBS (n = 15), MPTP (n = 38), MPTP + tolDC (n = 22), MPTP + mDC (n = 19), and MPTP + shClec5a (n = 11) groups. tolDCs and mDCs were generated by treatment with α-syn. (B) Plots depicting disease severity. Disease severity was graded on a scale of 0–10 ($^{++}p < 0.01$ vs. MPTP; **Supplementary Table 1**). (C) Immunofluorescence staining of the TH-positive neurons in the SNpc of mice. Representative photomicrographs of TH (a marker of dopamine neurons) in the SN region. Scale bar: top, 500 µm; bottom 100 µm. (D) Quantification of TH-positive neurons within the SN region (Kruskal–Wallis ANOVA; n = 3; $^{\#}p < 0.05$ vs. PBS). (E) Immunofluorescence staining of TH-positive neurons and α-syn in the SNpc of mice. Representative photomicrographs of TH and α-syn staining in the SN region. Scale bar: 50 µm. All microscopy images were obtained under consistent imaging parameters, and representative images are displayed. (F) Cytokine profile of the brain (Tukey–Kramer ANOVA; n $\geq$ 3; $^{+}p < 0.05$ vs. MPTP; $^{*}p < 0.05$ vs. MPTP + tolDC). (G) Pole test measuring descent time and reversal initiation (Kruskal–Wallis ANOVA; n $\geq$ 8; $^{\#\#}p < 0.01$, and $^{\#\#\#}p < 0.001$ vs. PBS; $^{*}p < 0.05$ vs. MPTP + tolDC). (H) Stepping test counting adjusted forelimb steps (Kruskal–Wallis ANOVA; n $\geq$ 6; $^{\#}p < 0.05$, $^{\#\#}p < 0.01$ and $^{\#\#\#}p < 0.001$ vs. PBS). (I) Tremor test evaluating tremor severity based on motion blur from stacked video frames (Kruskal–Wallis ANOVA; n $\geq$ 4 independent mice; $^{\#}p < 0.05$ vs. PBS). All data are expressed as the mean $\pm$ SD.

Tregs and $CD45^{+}CD11b^{+}CD206^{+}$ M2 macrophages were enhanced in the brains of PD mice following tolDC injection. Furthermore, in the MPTP + mDC group, the proportion of Tregs in the brain decreased, and that of $CD45^{+}CD11b^{+}CD86^{+}$ M1 macrophages significantly increased compared with the MPTP + tolDC mice. Such effects were not observed in the spleen (**Supplementary Fig. 4A**), although the proportion of Tregs in the submandibular LNs increased (**Supplementary Fig. 4B**). These results suggest that tolDCs may significantly reduce the number of M1 macrophages in the brain, potentially suppressing the excessive immune response in the CNS.

4. Discussion

PD is a progressive neurodegenerative disease characterized by dopaminergic neuron loss, motor dysfunction, and α-syn accumulation. Although current treatments provide only symptomatic relief, they do not prevent or reverse neurodegeneration. As inhibition of $CD4^{+}$ T cell proliferation via immune tolerance induction may suppress immune responses in PD [12–15], we hypothesized that tolDCs may also play a crucial role in CNS immunity. However, a major challenge in tolDC-based therapies is the lack of reliable functional markers to distinguish them from immunogenic mDCs, as both share surface molecules. This study investigated the applicability of Clec5a as a marker of the tolerogenic phenotype.

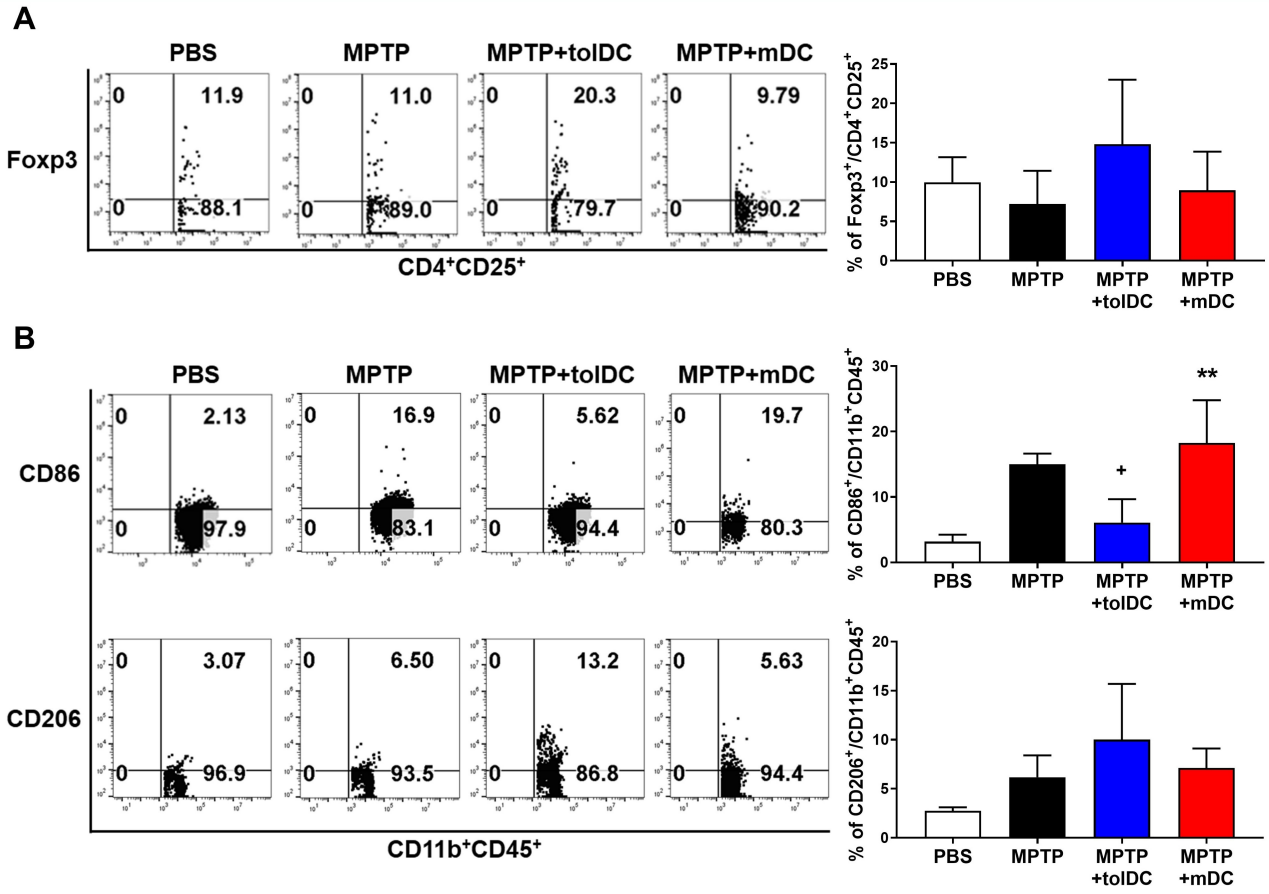

Fig. 6. tolDC-induced Treg infiltration and M2 macrophage differentiation in the brain. (A) The percentages of regulatory T cells (Tregs) ($CD4^+CD25^+Foxp3^+$) in the brain (Kruskal–Wallis ANOVA; $n \geq 3$). (B) The percentage of M1 ($CD45^+CD11b^+CD86^+$) and M2 ($CD45^+CD11b^+CD206^+$) macrophages in the brain (Kruskal–Wallis ANOVA; $n \geq 3$; $^{**}p < 0.01$ vs. MPTP + tolDC; $^{+}p < 0.05$ vs. MPTP). Leukocytes were isolated from perfused mouse brains on day 5 post-MPTP treatment and analyzed by flow cytometry. All data are expressed as the mean ± SD.

Clec5a was selectively upregulated in tolDCs, thereby increasing IL-10 and Treg differentiation, but decreasing IL-6 levels. Clec5a knockdown in tolDCs abrogated these effects, enhancing Th1 responses but impairing Treg generation, highlighting its essential role in shaping the immune balance. Clec5a mechanistically modulated two key signaling pathways: STAT3 and NF-κB. Clec5a knockdown reduced STAT3 phosphorylation but enhanced NF-κB p65 activation, without influencing the MAPK pathway components. Given the established roles of STAT3 in promoting tolerance and NF-κB in driving inflammation, these data suggest that Clec5a orchestrates the immune profile of tolDCs through the coordinated regulation of these pathways, although this reflects a correlative association rather than direct mechanistic evidence. This regulatory role contrasts with the well-established proinflammatory functions of Clec5a in other myeloid cells and suggests that its function may be context-dependent, influenced by the tolerogenic signaling milieu of tolDCs.

Crucially, the functional relevance of Clec5a-expressing tolDCs was confirmed *in vivo*. In this study, we specifically identified Treg and M1/M2 cells among the various brain cell types when assessing the impacts of tolDC. Clec5a-expressing tolDCs improved the pathological and behavioral impairments in the MPTP-induced PD model by regulating immune responses in the brain and reducing M1 macrophages but increasing Treg populations, which were associated with anti-inflammatory changes. Although we did not directly assess Treg suppressive function, the accompanying cytokine profile and behavioral improvements suggest their functional relevance. However, the MPTP mice injected with the Clec5a-knockdown tolDCs exhibited more severe pathogenesis and an accelerated loss of dopaminergic neurons. These observations provide compelling evidence that Clec5a plays a vital role in the neuroprotective activity of tolDCs. Although we did not investigate the direct interaction between tolDCs and microglia, the observed effects are likely mediated by peripherally induced Tregs. Exploring how these Tregs influence CNS-resident immune cells, such as microglia, would be an important direction for future studies.

From a translational perspective, DCs offer a unique therapeutic advantage in neurodegenerative diseases such as PD due to their dual roles in immune regulation and Ag presentation. This is supported by recent findings indicating that metabolic risk factors can affect treatment outcomes in PD models [47]. Compared with microglia, DCs are more effective in priming T cells and can migrate to lymphoid organs, making them superior candidates for CNS immune modulation [48,49]. Notably, α-syn-sensitized DCs induce Ag-specific immune responses without provoking systemic inflammation, supporting the DC-based Ag-specific immunotherapy of PD [50–54]. The "self-adjuvant" nature of DCs, combined with their autologous origin, minimizes the risk of immune rejection or off-target effects [55]. For future clinical applications, autologous monocyte-derived tolDCs may be preferred due to their low immunogenicity and established use in immunotherapy. Subcutaneous delivery near the axillary LNs—such as in the upper arm—could provide a practical route for promoting peripheral tolerance while minimizing the risk of autoimmune responses. Furthermore, our preliminary observation of elevated CLEC5A expression in human monocyte-derived tolDCs (data not shown) supports the potential biological relevance of this approach in human settings, although further validation is needed.

5. Conclusions

Our study provides evidence that Clec5a-expressing tolDCs play an important role in modulating neuroinflammation and promoting neuroprotection in a PD model. We demonstrated that Clec5a enhances IL-10 production and Treg populations while inhibiting NF-κB signaling, contributing to the tolerogenic function of tolDCs. The therapeutic potential of Clec5a-expressing tolDCs was further supported by observations in MPTP-intoxicated mice, where they alleviated pathological and behavioral impairments and preserved dopaminergic neurons. Notably, the knockdown of Clec5a accelerated disease progression, highlighting its functional relevance in PD pathogenesis. Taken together, these findings suggest that Clec5a may serve as a potential marker and immune modulator for DC-based strategies aimed at regulating neuroinflammation in PD.

Availability of Data and Materials

The data supporting the findings of this study are available within the article and **Supplementary Material**. All data was generated at the Department of Life Science of CHA University and is available from the corresponding authors upon reasonable request.

Author Contributions

SYC, JHN, and DSL conceived the study and designed the experiments; SYC, JHN, MSS, JHL, KEN, and JSO performed the experiments; NCJ, JYS, and DSL analyzed and interpreted the data; SYC, JHN, MSS, and DSL wrote the manuscript. All authors contributed to editorial changes in the manuscript. All authors read and approved the final manuscript. All authors have participated sufficiently in the work and agreed to be accountable for all aspects of the work.

Ethics Approval and Consent to Participate

All protocols involving the use of animals were reviewed and approved by the Institutional Animal Care and Use Committee of CHA University (Project IACUC210167), and all experiments were conducted in accordance with the relevant regulations and guidelines. Without performing carcinogenic procedures, animals will be euthanized using CO_2 gas solely for the purpose of collecting samples for DC generation. The PD mouse model will span a total period of two weeks from initiation to completion. The study will involve the minimum number of animals and a short experimental duration, with close monitoring of behavioral changes to determine appropriate humane endpoints. All animal experiments adhered to the 3R principles (Replacement, Reduction, Refinement).

Acknowledgment

Not applicable.

Funding

This research was supported by the Basic Science Research Program through the National Research Foundation of Korea (NRF), funded by the Ministry of Education (grant number: 2021R1I1A2045723).

Conflict of Interest

The authors declare no conflict of interest.

Supplementary Material

Supplementary material associated with this article can be found, in the online version, at https://doi.org/10.31083/FBL39570.

References

[1] Chaudhuri KR, Azulay JP, Odin P, Lindvall S, Domingos J, Alobaidi A, *et al*. Economic Burden of Parkinson's Disease: A Multinational, Real-World, Cost-of-Illness Study. Drugs - Real World Outcomes. 2024; 11: 1–11. https://doi.org/10.1007/s40801-023-00410-1.

[2] Huang Y, Liu Z, Cao BB, Qiu YH, Peng YP. Treg Cells Attenuate Neuroinflammation and Protect Neurons in a Mouse Model of Parkinson's Disease. Journal of Neuroimmune Pharmacology: the Official Journal of the Society on NeuroImmune Pharmacology. 2020; 15: 224–237. https://doi.org/10.1007/s11481-019-09888-5.

[3] Tansey MG, Wallings RL, Houser MC, Herrick MK, Keating CE, Joers V. Inflammation and immune dysfunction in Parkin-

son disease. Nature Reviews. Immunology. 2022; 22: 657–673. https://doi.org/10.1038/s41577-022-00684-6.

[4] van Rooden SM, Visser M, Verbaan D, Marinus J, van Hilten JJ. Patterns of motor and non-motor features in Parkinson's disease. Journal of Neurology, Neurosurgery, and Psychiatry. 2009; 80: 846–850. https://doi.org/10.1136/jnnp.2008.166629.

[5] Savica R, Carlin JM, Grossardt BR, Bower JH, Ahlskog JE, Maraganore DM, *et al*. Medical records documentation of constipation preceding Parkinson disease: A case-control study. Neurology. 2009; 73: 1752–1758. https://doi.org/10.1212/WNL.0b013e3181c34af5.

[6] Yao L, Lu F, Koc S, Zheng Z, Wang B, Zhang S, *et al*. LRRK2 Gly2019Ser Mutation Promotes ER Stress via Interacting with THBS1/TGF-β1 in Parkinson's Disease. Advanced Science (Weinheim, Baden-Wurttemberg, Germany). 2023; 10: e2303711. https://doi.org/10.1002/advs.202303711.

[7] Depboylu C, Stricker S, Ghobril JP, Oertel WH, Priller J, Höglinger GU. Brain-resident microglia predominate over infiltrating myeloid cells in activation, phagocytosis and interaction with T-lymphocytes in the MPTP mouse model of Parkinson disease. Experimental Neurology. 2012; 238: 183–191. https://doi.org/10.1016/j.expneurol.2012.08.020.

[8] Członkowska A, Kohutnicka M, Kurkowska-Jastrzebska I, Członkowski A. Microglial reaction in MPTP (1-methyl-4-phenyl-1,2,3,6-tetrahydropyridine) induced Parkinson's disease mice model. Neurodegeneration: a Journal for Neurodegenerative Disorders, Neuroprotection, and Neuroregeneration. 1996; 5: 137–143. https://doi.org/10.1006/neur.1996.0020.

[9] Joers V, Tansey MG, Mulas G, Carta AR. Microglial phenotypes in Parkinson's disease and animal models of the disease. Progress in Neurobiology. 2017; 155: 57–75. https://doi.org/10.1016/j.pneurobio.2016.04.006.

[10] McGeer PL, Itagaki S, Akiyama H, McGeer EG. Rate of cell death in parkinsonism indicates active neuropathological process. Annals of Neurology. 1988; 24: 574–576. https://doi.org/10.1002/ana.410240415.

[11] Lavisse S, Goutal S, Wimberley C, Tonietto M, Bottlaender M, Gervais P, *et al*. Increased microglial activation in patients with Parkinson disease using [^{18}F]-DPA714 TSPO PET imaging. Parkinsonism & Related Disorders. 2021; 82: 29–36. https://doi.org/10.1016/j.parkreldis.2020.11.011.

[12] Brochard V, Combadière B, Prigent A, Laouar Y, Perrin A, Beray-Berthat V, *et al*. Infiltration of CD4+ lymphocytes into the brain contributes to neurodegeneration in a mouse model of Parkinson disease. The Journal of Clinical Investigation. 2009; 119: 182–192. https://doi.org/10.1172/JCI36470.

[13] Chen Y, Qi B, Xu W, Ma B, Li L, Chen Q, *et al*. Clinical correlation of peripheral CD4+ cell sub sets, their imbalance and Parkinson's disease. Molecular Medicine Reports. 2015; 12: 6105–6111. https://doi.org/10.3892/mmr.2015.4136.

[14] Álvarez-Luquín DD, Guevara-Salinas A, Arce-Sillas A, Espinosa-Cárdenas R, Leyva-Hernández J, Montes-Moratilla EU, *et al*. Increased Tc17 cell levels and imbalance of naïve/effector immune response in Parkinson's disease patients in a two-year follow-up: a case control study. Journal of Translational Medicine. 2021; 19: 378. https://doi.org/10.1186/s12967-021-03055-2.

[15] Saunders JAH, Estes KA, Kosloski LM, Allen HE, Dempsey KM, Torres-Russotto DR, *et al*. CD4+ regulatory and effector/memory T cell subsets profile motor dysfunction in Parkinson's disease. Journal of Neuroimmune Pharmacology: the Official Journal of the Society on NeuroImmune Pharmacology. 2012; 7: 927–938. https://doi.org/10.1007/s11481-012-9402-z.

[16] Bhatia D, Grozdanov V, Ruf WP, Kassubek J, Ludolph AC, Weishaupt JH, *et al*. T-cell dysregulation is associated with disease severity in Parkinson's Disease. Journal of Neuroinflammation. 2021; 18: 250. https://doi.org/10.1186/s12974-021-02296-8.

[17] Yan Z, Yang W, Wei H, Dean MN, Standaert DG, Cutter GR, *et al*. Dysregulation of the Adaptive Immune System in Patients With Early-Stage Parkinson Disease. Neurology(R) Neuroimmunology & Neuroinflammation. 2021; 8: e1036. https://doi.org/10.1212/NXI.0000000000001036.

[18] Li J, Zhao J, Chen L, Gao H, Zhang J, Wang D, *et al*. α-Synuclein induces Th17 differentiation and impairs the function and stability of Tregs by promoting RORC transcription in Parkinson's disease. Brain, Behavior, and Immunity. 2023; 108: 32–44. https://doi.org/10.1016/j.bbi.2022.10.023.

[19] Thome AD, Atassi F, Wang J, Faridar A, Zhao W, Thonhoff JR, *et al*. Ex vivo expansion of dysfunctional regulatory T lymphocytes restores suppressive function in Parkinson's disease. NPJ Parkinson's Disease. 2021; 7: 41. https://doi.org/10.1038/s41531-021-00188-5.

[20] Baird JK, Bourdette D, Meshul CK, Quinn JF. The key role of T cells in Parkinson's disease pathogenesis and therapy. Parkinsonism & Related Disorders. 2019; 60: 25–31. https://doi.org/10.1016/j.parkreldis.2018.10.029.

[21] Pashenkov M, Teleshova N, Link H. Inflammation in the central nervous system: the role for dendritic cells. Brain Pathology (Zurich, Switzerland). 2003; 13: 23–33. https://doi.org/10.1111/j.1750-3639.2003.tb00003.x.

[22] Ludewig P, Gallizioli M, Urra X, Behr S, Brait VH, Gelderblom M, *et al*. Dendritic cells in brain diseases. Biochimica et Biophysica Acta. 2016; 1862: 352–367. https://doi.org/10.1016/j.bbadis.2015.11.003.

[23] Jansen MAA, Spiering R, Ludwig IS, van Eden W, Hilkens CMU, Broere F. Matured Tolerogenic Dendritic Cells Effectively Inhibit Autoantigen Specific CD4$^+$ T Cells in a Murine Arthritis Model. Frontiers in Immunology. 2019; 10: 2068. https://doi.org/10.3389/fimmu.2019.02068.

[24] Wan X, Bao L, Ma G, Long T, Li H, Zhang Y, *et al*. Tolerogenic dendritic cells alleviate collagen-induced arthritis by forming microchimerism and affecting the expression of immune checkpoint molecules. European Journal of Immunology. 2022; 52: 1980–1992. https://doi.org/10.1002/eji.202250068.

[25] Giannoukakis N, Phillips B, Finegold D, Harnaha J, Trucco M. Phase I (safety) study of autologous tolerogenic dendritic cells in type 1 diabetic patients. Diabetes Care. 2011; 34: 2026–2032. https://doi.org/10.2337/dc11-0472.

[26] Dáňová K, Grohová A, Strnadová P, Funda DP, Šumník Z, Lebl J, *et al*. Tolerogenic Dendritic Cells from Poorly Compensated Type 1 Diabetes Patients Have Decreased Ability To Induce Stable Antigen-Specific T Cell Hyporesponsiveness and Generation of Suppressive Regulatory T Cells. Journal of Immunology (Baltimore, Md.: 1950). 2017; 198: 729–740. https://doi.org/10.4049/jimmunol.1600676.

[27] Derdelinckx J, Mansilla MJ, De Laere M, Lee WP, Navarro-Barriuso J, Wens I, *et al*. Clinical and immunological control of experimental autoimmune encephalomyelitis by tolerogenic dendritic cells loaded with MOG-encoding mRNA. Journal of Neuroinflammation. 2019; 16: 167. https://doi.org/10.1186/s12974-019-1541-1.

[28] Xie Z, Chen J, Zheng C, Wu J, Cheng Y, Zhu S, *et al*. 1,25-dihydroxyvitamin D_3 -induced dendritic cells suppress experimental autoimmune encephalomyelitis by increasing proportions of the regulatory lymphocytes and reducing T helper type 1 and type 17 cells. Immunology. 2017; 152: 414–424. https://doi.org/10.1111/imm.12776.

[29] Zhu R, Sun H, Yu K, Zhong Y, Shi H, Wei Y, *et al*. Interleukin-37 and Dendritic Cells Treated With Interleukin-37 Plus Troponin I Ameliorate Cardiac Remodeling After Myocardial Infarction. Journal of the American Heart Association. 2016; 5: e004406.

https://doi.org/10.1161/JAHA.116.004406.
[30] Wang Q, Chen Z, Guo J, Peng X, Zheng Z, Chen H, *et al*. Atorvastatin-induced tolerogenic dendritic cells improve cardiac remodeling by suppressing TLR-4/NF-κB activation after myocardial infarction. Inflammation Research: Official Journal of the European Histamine Research Society ... [et Al.]. 2023; 72: 13–25. https://doi.org/10.1007/s00011-022-01654-3.
[31] Lee EG, Jung NC, Lee JH, Song JY, Ryu SY, Seo HG, *et al*. Tolerogenic dendritic cells show gene expression profiles that are different from those of immunogenic dendritic cells in DBA/1 mice. Autoimmunity. 2016; 49: 90–101. https://doi.org/10.3109/08916934.2015.1124424.
[32] Takaki R, Watson SR, Lanier LL. DAP12: an adapter protein with dual functionality. Immunological Reviews. 2006; 214: 118–129. https://doi.org/10.1111/j.1600-065X.2006.00466.x.
[33] Hamerman JA, Lanier LL. Inhibition of immune responses by ITAM-bearing receptors. Science's STKE: Signal Transduction Knowledge Environment. 2006; 2006: re1. https://doi.org/10.1126/stke.3202006re1.
[34] Fuchs A, Cella M, Kondo T, Colonna M. Paradoxic inhibition of human natural interferon-producing cells by the activating receptor NKp44. Blood. 2005; 106: 2076–2082. https://doi.org/10.1182/blood-2004-12-4802.
[35] Tong L, Li J, Choi J, Pant A, Xia Y, Jackson C, *et al*. CLEC5A expressed on myeloid cells as a M2 biomarker relates to immunosuppression and decreased survival in patients with glioma. Cancer Gene Therapy. 2020; 27: 669–679. https://doi.org/10.1038/s41417-019-0140-8.
[36] Bakker AB, Baker E, Sutherland GR, Phillips JH, Lanier LL. Myeloid DAP12-associating lectin (MDL)-1 is a cell surface receptor involved in the activation of myeloid cells. Proceedings of the National Academy of Sciences of the United States of America. 1999; 96: 9792–9796. https://doi.org/10.1073/pnas.96.17.9792.
[37] Tosiek MJ, Groesser K, Pekcec A, Zwirek M, Murugesan G, Borges E. Activation of the Innate Immune Checkpoint CLEC5A on Myeloid Cells in the Absence of Danger Signals Modulates Macrophages' Function but Does Not Trigger the Adaptive T Cell Immune Response. Journal of Immunology Research. 2022; 2022: 9926305. https://doi.org/10.1155/2022/9926305.
[38] Fan HW, Ni Q, Fan YN, Ma ZX, Li YB. C-type lectin domain family 5, member A (CLEC5A, MDL-1) promotes brain glioblastoma tumorigenesis by regulating PI3K/Akt signalling. Cell Proliferation. 2019; 52: e12584. https://doi.org/10.1111/cpr.12584.
[39] Santoro M, Fadda P, Klephan KJ, Hull C, Teismann P, Platt B, *et al*. Neurochemical, histological, and behavioral profiling of the acute, sub-acute, and chronic MPTP mouse model of Parkinson's disease. Journal of Neurochemistry. 2023; 164: 121–142. https://doi.org/10.1111/jnc.15699.
[40] Yao L, Ye Y, Mao H, Lu F, He X, Lu G, *et al*. MicroRNA-124 regulates the expression of MEKK3 in the inflammatory pathogenesis of Parkinson's disease. Journal of Neuroinflammation. 2018; 15: 13. https://doi.org/10.1186/s12974-018-1053-4.
[41] Yao L, Zhu Z, Wu J, Zhang Y, Zhang H, Sun X, *et al*. MicroRNA-124 regulates the expression of p62/p38 and promotes autophagy in the inflammatory pathogenesis of Parkinson's disease. FASEB Journal: Official Publication of the Federation of American Societies for Experimental Biology. 2019; 33: 8648–8665. https://doi.org/10.1096/fj.201900363R.
[42] Lim DS, Kang MS, Jeong JA, Bae YS. Semi-mature DC are immunogenic and not tolerogenic when inoculated at a high dose in collagen-induced arthritis mice. European Journal of Immunology. 2009; 39: 1334–1343. https://doi.org/10.1002/eji.200838987.
[43] Jackson-Lewis V, Przedborski S. Protocol for the MPTP mouse model of Parkinson's disease. Nature Protocols. 2007; 2: 141–151. https://doi.org/10.1038/nprot.2006.342.
[44] Phillips KA, Ross CN, Spross J, Cheng CJ, Izquierdo A, Biju KC, *et al*. Behavioral phenotypes associated with MPTP induction of partial lesions in common marmosets (Callithrix jacchus). Behavioural Brain Research. 2017; 325: 51–62. https://doi.org/10.1016/j.bbr.2017.02.010.
[45] Koprich JB, Reske-Nielsen C, Mithal P, Isacson O. Neuroinflammation mediated by IL-1beta increases susceptibility of dopamine neurons to degeneration in an animal model of Parkinson's disease. Journal of Neuroinflammation. 2008; 5: 8. https://doi.org/10.1186/1742-2094-5-8.
[46] Barcia C, Ros CM, Annese V, Gómez A, Ros-Bernal F, Aguado-Yera D, *et al*. IFN-γ signaling, with the synergistic contribution of TNF-α, mediates cell specific microglial and astroglial activation in experimental models of Parkinson's disease. Cell Death & Disease. 2011; 2: e142. https://doi.org/10.1038/cddis.2011.17.
[47] Yao L, Chen R, Zheng Z, Hatami M, Koc S, Wang X, *et al*. Translational evaluation of metabolic risk factors impacting DBS efficacy for PD-related sleep and depressive disorders: preclinical, prospective and cohort studies. International Journal of Surgery (London, England). 2025; 111: 543–566. https://doi.org/10.1097/JS9.0000000000002081.
[48] Xiao BG, Huang YM, Yang JS, Xu LY, Link H. Bone marrow-derived dendritic cells from experimental allergic encephalomyelitis induce immune tolerance to EAE in Lewis rats. Clinical and Experimental Immunology. 2001; 125: 300–309. https://doi.org/10.1046/j.1365-2249.2001.01573.x.
[49] Aloisi F, Ria F, Columba-Cabezas S, Hess H, Penna G, Adorini L. Relative efficiency of microglia, astrocytes, dendritic cells and B cells in naive CD4+ T cell priming and Th1/Th2 cell restimulation. European Journal of Immunology. 1999; 29: 2705–2714. https://doi.org/10.1002/(SICI)1521-4141(199909)29:09<2705::AID-IMMU2705>3.0.CO;2-1.
[50] Serot JM, Béné MC, Foliguet B, Faure GC. Monocyte-derived IL-10-secreting dendritic cells in choroid plexus epithelium. Journal of Neuroimmunology. 2000; 105: 115–119. https://doi.org/10.1016/s0165-5728(99)00240-4.
[51] Yanamandra K, Gruden MA, Casaite V, Meskys R, Forsgren L, Morozova-Roche LA. α-synuclein reactive antibodies as diagnostic biomarkers in blood sera of Parkinson's disease patients. PloS One. 2011; 6: e18513. https://doi.org/10.1371/journal.pone.0018513.
[52] Huang YR, Xie XX, Ji M, Yu XL, Zhu J, Zhang LX, *et al*. Naturally occurring autoantibodies against α-synuclein rescues memory and motor deficits and attenuates α-synuclein pathology in mouse model of Parkinson's disease. Neurobiology of Disease. 2019; 124: 202–217. https://doi.org/10.1016/j.nbd.2018.11.024.
[53] Romero-Ramos M, von Euler Chelpin M, Sanchez-Guajardo V. Vaccination strategies for Parkinson disease: induction of a swift attack or raising tolerance? Human Vaccines & Immunotherapeutics. 2014; 10: 852–867. https://doi.org/10.4161/hv.28578.
[54] Ugen KE, Lin X, Bai G, Liang Z, Cai J, Li K, *et al*. Evaluation of an α synuclein sensitized dendritic cell based vaccine in a transgenic mouse model of Parkinson disease. Human Vaccines & Immunotherapeutics. 2015; 11: 922–930. https://doi.org/10.1080/21645515.2015.1012033.
[55] Hart DN. Dendritic cells: unique leukocyte populations which control the primary immune response. Blood. 1997; 90: 3245–3287.